

The Unified PWM Implementation Method for Three-Phase Inverters

Xiao-ling Wen and Xiang-gen Yin

College of Electrical and Electronic Engineering, Huazhong University of Science and Technology

430074 Wuhan, Hubei, China

Abstract-The three-phase inverter with the conventional space-vector pulse width modulation (SVPWM) algorithm has fast dynamic response, but the complex coordinate transformations, trigonometric function calculations, and sector number identification should be performed. In this paper, the relationship between SVPWM and three-phase carrier-based PWM is comprehensively analyzed. A zero-vector distribution variable k_1 , which changes from zero to one, is introduced, and the influence of k_1 on characteristics of the PWM is investigated. The continuous SVPWM is generated when $0 < k_1 < 1$, and several typical kinds of discontinuous SVPWM are generated when $k_1 = 1$ or 0. The sinusoidal PWM (SPWM) and all kinds of SVPWM are unified in a modulation function expression, and it is proved that SVPWM is a zero-sequence voltage signal injection carrier-based PWM in effect. Moreover, a unified PWM fast algorithm is proposed, and it has only normal arithmetic operations and needn't identify the sector to which the voltage reference signal belongs. The SPWM and all SVPWM methods can easily be implemented using the developed algorithm. The algorithm has the advantage of the conventional SVPWM algorithm with fast dynamic response and needs less computation time. The simulation and experiment results show that the proposed method is valid and feasible.

Index Terms-Carrier-based PWM, space vector PWM, fast algorithm, harmonic analysis.

I. INTRODUCTION

For a long period, carrier-based pulse-width modulation (PWM) method [1], [2] was widely used in most applications. With the development of microprocessors, space vector pulse-width modulation (SVPWM) [3] has become one of the most popular PWM methods for three-phase converters. Although the two PWM methods have been developed from entirely different points of view, they are equivalent under special circumstances. Therefore, many attempts have been made to unite the two types of PWM methods. In Ref. [4] and [5], the implicit modulating functions of the discontinuous SVPWM technique with minimum switching losses were presented. The relationship between space vectors and fundamental modulation signals was derived in [6-9] where it

was shown that the SVPWM method was a zero-sequence signal injection carrier-based PWM method in effect and the freedom in selecting the distribution of the two zero-vectors in the SVPWM technique is equivalent to the freedom in selecting the zero-sequence signal in the carrier-based PWM technique. Furthermore, simple methods for generating the zero-sequence signals of classical SVPWM and several discontinuous SVPWM by the magnitude test are described in [9]. However, it has not yet been reported that all kinds of the existing continuous and discontinuous PWM methods are intuitively embodied in a modulation function expression.

An aptitude for easy digital implementation and wide linear modulation range for output line-to-line voltages are the notable features of SVPWM, but the implementation of the SVPWM method with a direct digital technique is formidable when applied in the actual field because the complex coordinate transformations, trigonometric function calculations, sector number identification, and a recombination process for actual gating times should be performed [3], [10]. A unified voltage modulation technique is proposed in [11] where the actual gating times for each inverter arm are simply deduced by using the “effective time” relocation algorithm, and the operating fashion of the proposed scheme can be easily changed to sinusoidal PWM (SPWM), classical SVPWM, and discontinuous modulation schemes, but the authors did not consider all the existing continuous and discontinuous modulation schemes.

In this paper, the relationship between SVPWM and carrier-based PWM is comprehensively analyzed. A zero-vector distribution variable k_1 , which changes from zero to one, is introduced, and the influence of k_1 on harmonic characteristics of the PWM is investigated. In particular, SPWM, continuous SVPWM, and discontinuous SVPWM methods are explicitly united in a modulation function expression. Furthermore, a unified PWM fast algorithm is proposed, and it has only normal arithmetic operation and needn't identify the sector number.

II. SVPWM PRINCIPLE

The three-phase PWM inverter shown in Fig.1 is characterized by eight switching states of which six [$V_1(100)$ - $V_6(101)$] are active to form a hexagon, and two [$V_0(000)$ and

$V_7(111)$] are zero states that lie at the origin. The applying times of the voltage vectors V_0, V_1, \dots, V_7 are defined as t_0, t_1, \dots, t_7 . If a reference voltage vector V_r is given in the hexagon area, as shown in Fig.1(b), by employing space vector theory, the applying time of the two adjacent active vectors V_k and V_{k+1} ($k+1=1$ when $k=6$) and the total zero-voltage applying time are directly calculated in the following:

$$t_k = \sqrt{3}T_s[V_\alpha \sin(k\pi/3) - V_\beta \cos(k\pi/3)]/V_{dc}$$

$$t_{k+1} = \sqrt{3}T_s[V_\beta \cos((k-1)\pi/3) - V_\alpha \sin((k-1)\pi/3)]/V_{dc} \quad (1)$$

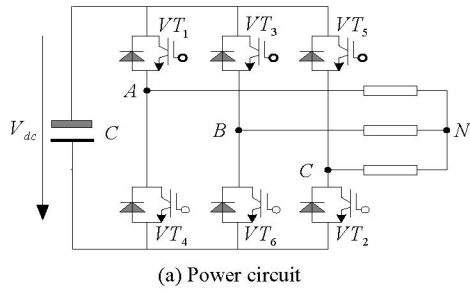
$$T_0 = T_s - t_k - t_{k+1}$$

where $V_\alpha = V_r \cdot \cos(\theta)$, $V_\beta = V_r \cdot \sin(\theta)$, $\theta = \delta + (k-1)\pi/3$, k =sector number ($1,2,\dots,6$), T_s is the sampling time, and V_{dc} is the dc-link voltage. The zero-voltage applying times can be written as

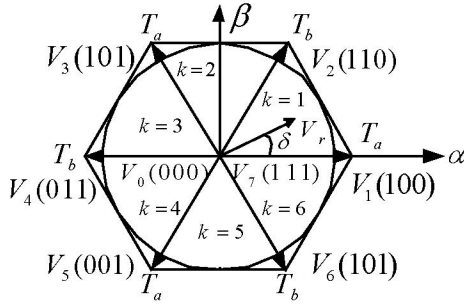
$$t_0 = k_1 \cdot T_0$$

$$t_7 = (1-k_1) \cdot T_0 \quad 0 \leq k_1 \leq 1 \quad (2)$$

where k_1 is a zero-vector distribution variable. The different distribution of t_0 and t_7 for zero-vectors yields different SVPWM schemes. The continuous SVPWM (which is called CPWM here.) is obtained when $0 < k_1 < 1$, and the discontinuous SVPWM (which is called DPWM.) is derived when $k_1=1$ or $k_1=0$. Furthermore, the SVPWM are classified as CPWM ($0 < k_1 < 1$), classical SVPWM ($k_1=0.5$), DPWMMAX ($k_1=0$), DPWMMIN ($k_1=1$), DPWM0 and DPWM1 (k_1 changes from zero to one at the ends of sectors.), and DPWM2 and DPWM3 (k_1 changes from zero to one in the middle of sectors.) [6], [9].



(a) Power circuit



(b) The space-vector diagram

Fig.1. Three-phase PWM inverter.

III. UNIFIED PWM FAST ALGORITHM

The relationship between the carrier-based PWM and SVPWM in sector 1 is illustrated in Fig.2. In the figure, unity triangle carrier wave gain is assumed and all the voltages are

normalized to $V_{dc}/2$. If the modulation index M is defined as the ratio of the reference phase voltage amplitude V_r to $V_{dc}/2$, the unified PWM modulation function can be expressed as [7], [8]

$$v_i^* = v_{ri}^* + v_z^*$$

$$v_n^* = M \cos[\theta - 2(m-1)\pi/3], i \in \{a, b, c\}, m \in \{1, 2, 3\} \quad (3)$$

$$v_{ix}^* = v_n^*(\theta - \pi/6)$$

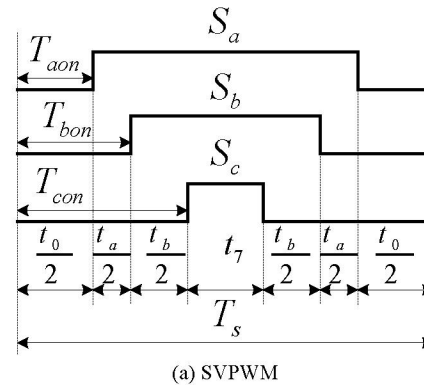
where v_z^* is the zero-sequence voltage signal, $v_z^* = 0$ for SPWM. For CPWM, v_z^* is as follows:

$$v_z^* = (1-2k_1) - (1-k_1)v_{max}^* - k_1v_{min}^*. \quad (4)$$

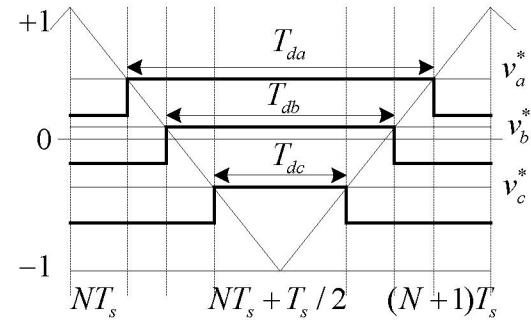
For discontinuous SVPWM, v_z^* is given by

$$v_z^* = \begin{cases} 1-v_{max}^* & \begin{cases} DPWM0 : |v_{max,x}^*| < |v_{min,x}^*| \\ DPWM1 : |v_{max,x}^*| \geq |v_{min,x}^*| \\ DPWM2 : |v_{max}^*| \geq |v_{min}^*| \\ DPWM3 : |v_{max}^*| < |v_{min}^*| \\ DPWMMAX \end{cases} \\ -1-v_{min}^* & \begin{cases} DPWM0 : |v_{max,x}^*| \geq |v_{min,x}^*| \\ DPWM1 : |v_{max,x}^*| < |v_{min,x}^*| \\ DPWM2 : |v_{max}^*| < |v_{min}^*| \\ DPWM3 : |v_{max}^*| \geq |v_{min}^*| \\ DPWMMIN \end{cases} \end{cases} \quad (5)$$

where $v_{max}^* = \max\{v_{ra}^*, v_{rb}^*, v_{rc}^*\}$, $v_{min}^* = \min\{v_{ra}^*, v_{rb}^*, v_{rc}^*\}$, $v_{max,x}^* = \max\{v_{ax}^*, v_{bx}^*, v_{cx}^*\}$, $v_{min,x}^* = \min\{v_{ax}^*, v_{bx}^*, v_{cx}^*\}$.



(a) SVPWM



(b) Carrier-based PWM

Fig.2. PWM switching signals.

According to Fig.2, in a sampling period, the actual gating times can be given by [6-8]

$$\begin{aligned} T_{di} &= T_s(1+v_i^*)/2 \\ T_{ion} &= (T_s - T_{di})/2 \quad i \in \{a, b, c\} \end{aligned} \quad (6)$$

From the equations (3)~(6), the gating times are deduced as follows:

$$T_{di} = \frac{T_s}{2}v_{ri}^* + T_e \quad i \in \{a, b, c\} \quad (7)$$

where T_e is called the offset time[11], and it can be expressed as

$$T_e = \begin{cases} T_s/2 & \text{for SPWM} \\ (1-k_1)T_s - (1-k_1)T_{max} - k_1T_{min} & \text{for CPWM} \end{cases} \quad (8)$$

$$T_e = \begin{cases} T_s - T_{max} & \begin{cases} DPWM0 : T_{max,x} + T_{min,x} < 0 \\ DPWM1 : T_{max,x} + T_{min,x} \geq 0 \\ DPWM2 : T_{max} + T_{min} \geq 0 \\ DPWM3 : T_{max} + T_{min} < 0 \\ DPWMMAX \end{cases} \\ -T_{min} & \begin{cases} DPWM0 : T_{max,x} + T_{min,x} < 0 \\ DPWM1 : T_{max,x} + T_{min,x} \geq 0 \\ DPWM2 : T_{max} + T_{min} \geq 0 \\ DPWM3 : T_{max} + T_{min} < 0 \\ DPWMMIN \end{cases} \end{cases} \quad (9)$$

where $T_{max} = v_{max}^* T_s / 2$, $T_{min} = v_{min}^* T_s / 2$, $T_{max,x} = v_{max,x}^* T_s / 2$, $T_{min,x} = v_{min,x}^* T_s / 2$. As is widely known, in order to guarantee the linearity of the inverter output voltage, the reference voltage vector should reside in the hexagon region. However, if the reference voltage vector exceeds the hexagon area (i.e. $T_{max} - T_{min} > T_s$), a commonly used simple over-modulation strategy is adopted, and the offset time is as follows:

$$T_e = -T_{min} T_s / (T_{max} - T_{min}) \quad (10)$$

Therefore, the equivalent relationship between SVPWM and the carrier-based PWM is established on the basis of the formula (3)~(10). Meanwhile, a unified PWM fast algorithm, in which the three phase reference voltages are used to calculate the actual gating times for each inverter arm directly, is derived.

IV. SIMULATION AND EXPERIMENTAL RESULTS

The simulation model for unified PWM method can be easily established according to (3)~(5). The various modulation features of the unified PWM method are simulated with the help of MATLAB/SIMULINK, and the simulation results are delineated in Fig.3. In this figure, the triangular carrier frequency is 1050Hz, the frequency of reference voltage is 50Hz, and the modulation index M is 1. Inspection of the discontinuous modulating function and switching signals of Fig.3 reveals that each output of the inverter arms is alternately left on the positive or negative rail of the dc-link voltage for 120° intervals of the fundamental period, and the average switching frequency and losses can be reduced by 33% [12]. In particular, the most efficient operation of the inverter

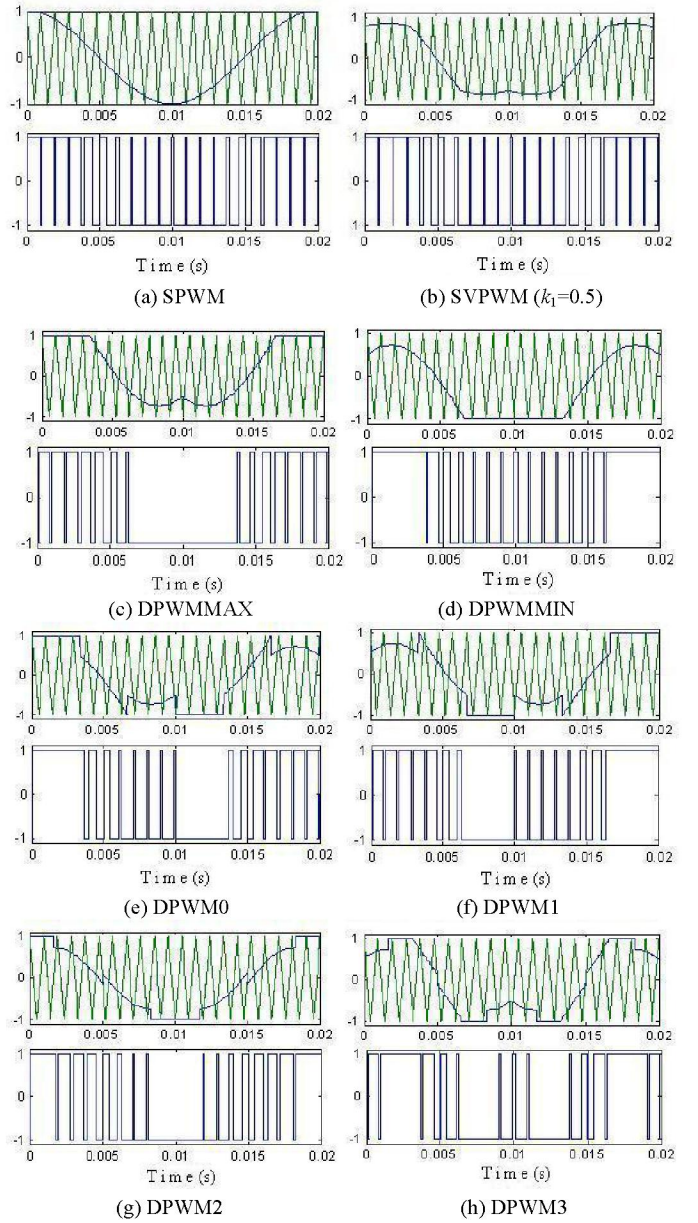


Fig.3. Triangle intersection PWM phase "a" modulation and switching signals.

corresponds to the load angle of 30°, such as an ac motor, when DPWM0 strategy is used. In this case, individual phase currents are not switched when passing through their peaks, and the highest switching losses are avoided.

On the basis of the unified PWM fast algorithm, a PWM controller, which consists of TMS320VC33 and FPGA, has been developed. By loading the pre-calculated gating times (T_{aon} , T_{bon} , T_{con}) to each counter at every sampling time, the gating sequence runs automatically for the proper inverter action. The gating circuit is implemented on a programmable logic device (FPGA). The switching signals of phase "a" and "b", which are measured by using the oscilloscope TDS3012B, are shown in Figs.4-10. Comparing Fig.3 with Figs.4-10, good

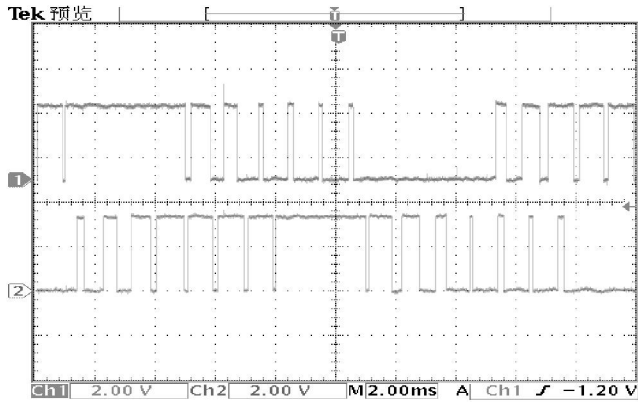


Fig.4. DPWM0 switching signals of phase “a” and “b”.

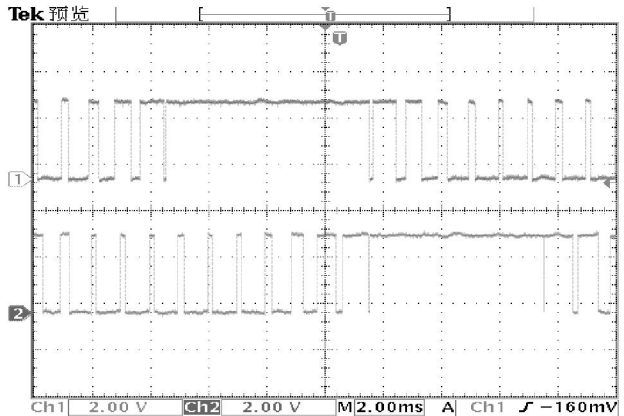


Fig.8. DPWMMAX switching signals of phase “a” and “b”.

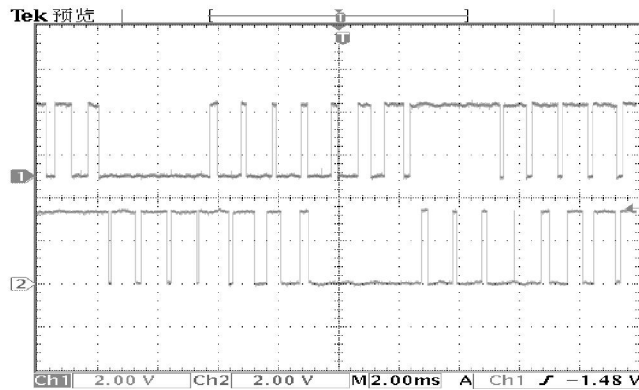


Fig.5. DPWM1 switching signals of phase “a” and “b”.

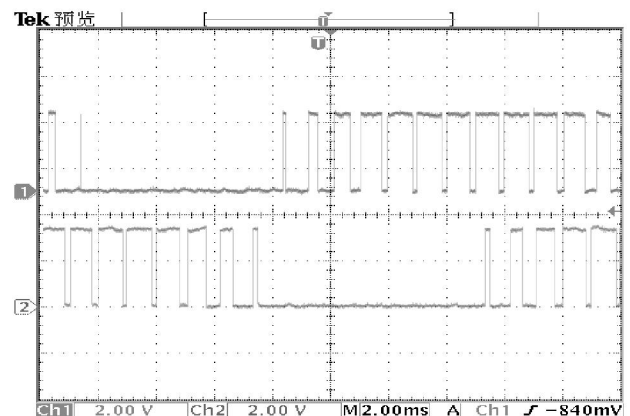


Fig.9. DPWMMIN switching signals of phase “a” and “b”.

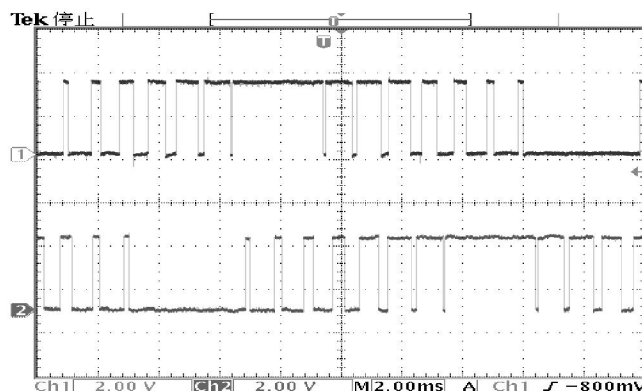


Fig.6. DPWM2 switching signals of phase “a” and “b”.

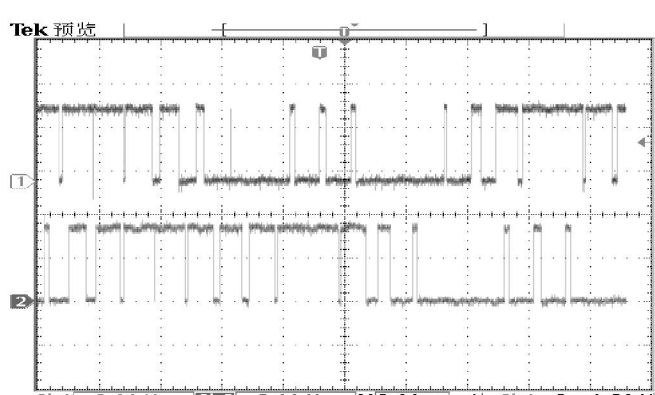


Fig.7. DPWM3 switching signals of phase “a” and “b”.

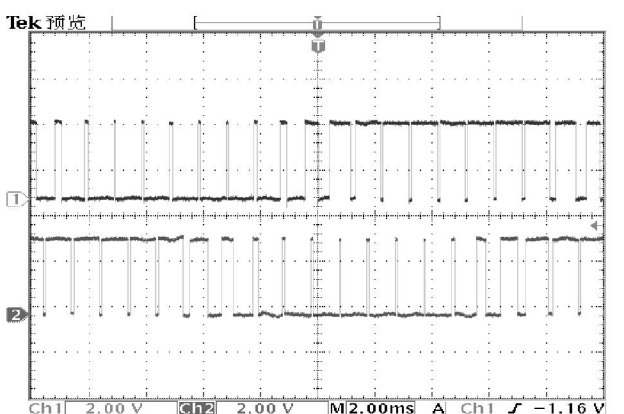


Fig.10. SVPWM ($k_1=0.5$) switching signals of phase “a” and “b”.

agreement between the simulation and experimental results can be observed.

The simplest measure of quality of voltage and currents of an inverter is the total harmonic distortion (THD) defined as the per-cent ratio of the harmonic component to the fundamental value of the voltage or current. Therefore, the output voltage(which is a pulse waveform without output filters.) and current spectra of the three-phase inverter are analyzed in order to compare the harmonic characteristics of the PWM strategies. The curves of the output voltage and current THD varying with the modulation index M for several typical PWM strategies are

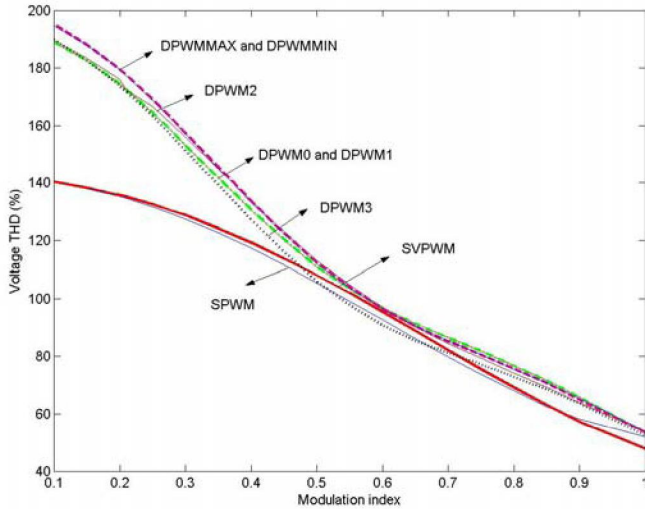


Fig.11. The line-to-line voltage THD for eight PWM strategies.

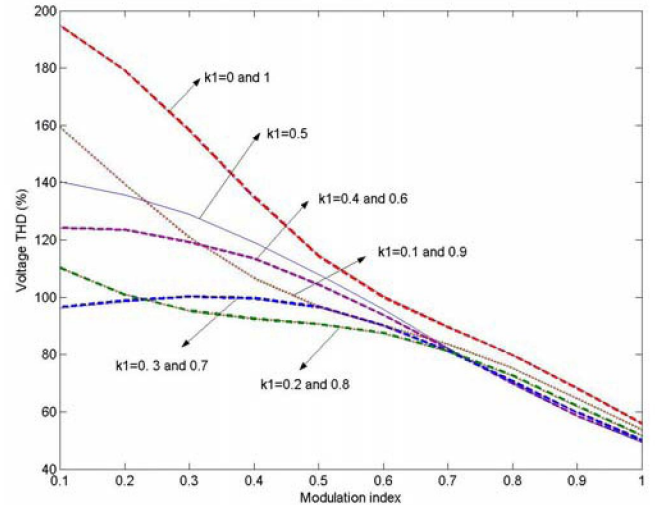


Fig.14. Curves of voltage THD varying with M when k_1 is constant.

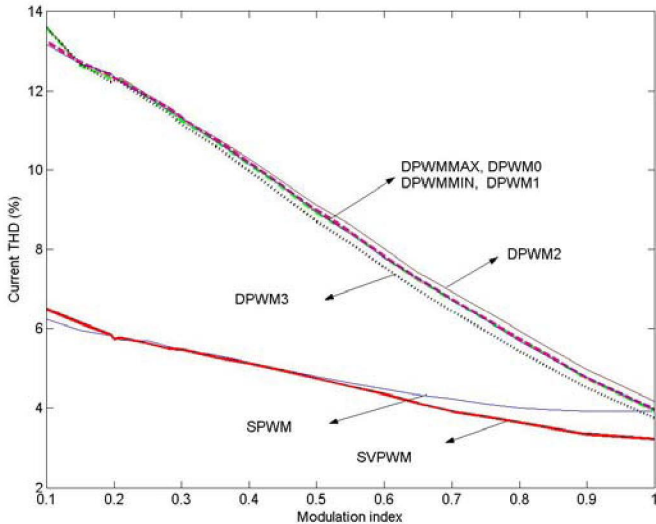


Fig.12. The phase current THD for eight PWM strategies.

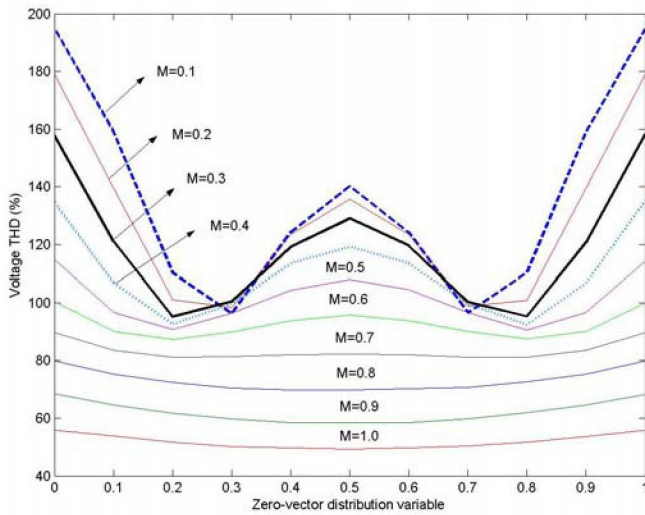


Fig.13. Curves of voltage THD varying with k_1 when M is constant.

illustrated in Figs. 11 and 12. Figs. 13 and 14 show the curves of the output voltage THD varying with the modulation M and zero-vector distribution variable k_1 for CPWM methods. In these figures, the sampling frequency is 1050Hz, the frequency of reference voltage is 50 Hz, the dc-link voltage is 300V, and a resistive-inductive load with $R=5 \Omega$ and $L=0.01H$ is used. As the figures indicate, the CPWM methods have lower harmonic distortion than the DPWM methods under the same conditions, and the difference is more pronounced at low M . However, as the modulation index increases, the voltage and current THD for DPWM schemes decrease greatly and are gradually close to those when CPWM schemes are used. Meanwhile, from Figs. 11 and 12, it can be seen that the DPWM3 is superior to the other DPWM schemes in the harmonic characteristics, SVPWM has lower voltage harmonic distortion than SPWM when $M>0.8$, and SPWM is inferior to SVPWM in the current harmonic performance when $M>0.2$. Figs. 13 and 14 indicate that the influence of k_1 on the harmonic characteristics of the CPWM strategies is great in the low modulation range but small in the high modulation range, and the CPWM with $k_1=0.5$ (i.e. classical SVPWM) has the lowest voltage THD when $M>0.7$.

V. CONCLUSION

A fast algorithm suitable for analog and digital implementation of the unified PWM method for three-phase inverters has been developed according to the relationship between carrier PWM and SVPWM strategies, and it is used to investigate the influence of the zero-vector distribution factor k_1 and modulation index M on the harmonic characteristics of different PWM methods. The simulation and experimental results show that the proposed method is feasible and valid.

It is shown that SPWM and SVPWM in low modulation and DPWM methods (especially DPWM0 for an ac drive and DPWM2 for the inverter with resistive load) in the high modulation range have superior performance in view of the

switching losses and harmonic characteristics. The unified PWM fast algorithm not only has the advantage of the direct digital PWM algorithm with fast dynamic response, but also can be more easily implemented with a microprocessor or DSP because three-phase reference voltages are directly used to calculate the actual gating times. Meanwhile, the explicit modulating function, which unites SPWM and all kinds of the existing SVPWM methods, is a very effective tool for the simulation and analysis of various modulation methods duo to its simplicity and intuition.

REFERENCES

- [1] S. R. Bowes, "New Sinusoidal Pulsewidth-Modulated Inverter," *Proc. Inst. Elect. Eng.*, vol. 122, no. 11, pp. 1279-1285, 1975.
- [2] S. R. Bowes and R. R. Clements, "Computer Aided Design of PWM inverter systems," *Proc. Inst. Elect. Eng.*, vol. 129, pt. B, no. 1, pp. 1-17, 1982.
- [3] H. W. van der Broeck, H. C. Skudelny, and G. V. Stanke, "Analysis and Realization of a pulse width modulator based on voltage space vector," *IEEE Trans. Ind. Applicat.*, vol. 24, pp. 142-150, Jan./Feb. 1988.
- [4] A. M. Trzynadlowski, R. L. Kirlin, and S. F. Legowski, "Space Vector PWM Technique with minimum switching losses and a variable pulse rate," *IEEE Trans. Ind. Electron.*, vol. 44, pp. 173-181, Apr. 1997.
- [5] A. M. Trzynadlowski and S. F. Legowski, "Minimum-Loss Vector PWM Strategy for Three-Phase Inverters," *IEEE Trans. Power Electron.*, vol. 9, pp. 26-34, Jan. 1994.
- [6] S. R. Bowes and Y. S. Lai, "The Relationship between Space-Vector Modulation and Regular-Sampled PWM," *IEEE Trans. Ind. Electron.*, vol. 44, pp. 670-679, Oct. 1997.
- [7] V. Blasko, "Analysis of Hybrid PWM based on modified space-vector and triangle-comparison methods," *IEEE Trans. Ind. Applicat.*, vol. 33, pp. 756-764, May/June 1997.
- [8] Keliang Zhou and Danwei Wang, "Relationship between space-vector modulation and three-phase carrier-based PWM: A Comprehensive Analysis," *IEEE Trans. Ind. Electron.*, vol. 49, pp. 186-195, Feb. 2002.
- [9] A. M. Hava, R. J. Kerkmen, and T. A. Lipo, "Simple Analytical and Graphical Methods for Carrier-Based PWM-VSI Drives," *IEEE Trans. Power Electron.*, vol. 14, pp. 49-61, Jan. 1999.
- [10] J. O. Pinto, B. K. Bose, Luiz Eduardo Borges da Silva, and Marian P. Kazmierkowski, "A Neural-Network-Based Space-Vector PWM Controller for Voltage-Fed Inverter Induction Motor Drive," *IEEE Trans. Ind. Applicat.*, vol. 36, pp. 1628-1636, Nov./Dec. 2000.
- [11] D. W. Chung, J. S. Kim, and S. K. Sul, "Unified Voltage Modulation Technique for Real-Time Three-Phase Power Conversion," *IEEE Trans. Ind. Applicat.*, vol. 34, pp. 374-380, Mar./Apr. 1998.
- [12] J. W. Kolar, H. Ertl, and F. C. Zach, "Influence of the modulation method on the Conduction and Switching Losses of a PWM converter system," *IEEE Trans. Ind. Applicat.*, vol. 27, pp. 1603-1075, Nov./Dec. 1998.